

# Combinatorial and Chemotopic Odorant Coding in the Zebrafish Olfactory Bulb Visualized by Optical Imaging

Rainer W. Friedrich and Sigrun I. Korsching\*

Max-Planck-Institut für Entwicklungsbiologie

Abteilung Physikalische Biologie

D-72076 Tübingen

Federal Republic of Germany

## Summary

Odors are thought to be represented by a distributed code across the glomerular modules in the olfactory bulb (OB). Here, we optically imaged presynaptic activity in glomerular modules of the zebrafish OB induced by a class of natural odorants (amino acids [AAs]) after labeling of primary afferents with a calcium-sensitive dye. AAs induce complex combinatorial patterns of active glomerular modules that are unique for different stimuli and concentrations. Quantitative analysis shows that defined molecular features of stimuli are correlated with activity in spatially confined groups of glomerular modules. These results provide direct evidence that identity and concentration of odorants are encoded by glomerular activity patterns and reveal a coarse chemotopic organization of the array of glomerular modules.

## Introduction

How the nervous system recognizes and distinguishes between a vast number of odors is an intriguing problem. Olfactory stimuli are transduced into electrical activity by olfactory receptor neurons (ORNs), which send a single unbranched axon to the first relay station in the central nervous system, the OB. ORN axons synapse onto mitral cells (and tufted cells, in higher vertebrates) and local interneurons in spherical neuropil structures, the olfactory glomeruli. Glomeruli are histologically distinct units in most species and are thought to function as basic modules in information processing (Shepherd, 1994). Mitral cell axons exit the OB and project to several higher brain areas, most of which are telencephalic (Satou, 1992; Shipley and Ennis, 1996). In addition, mitral cells as well as local interneurons form extensive lateral connections within the OB. The functions of these connections involve lateral inhibition, which could refine the spatial and temporal patterns of output activity carried by mitral and/or tufted cells (Scott et al., 1993; Yokoi et al., 1995).

How is odor information encoded in the OB? Nonpheromone odorants usually induce nonhomogenous distributions of neuronal activity in the OB that exhibit some stimulus specificity, indicating that odorants are processed through a distributed code rather than through single labeled lines (Adrian, 1953; Moulton, 1967; Stewart et al., 1979; Kauer, 1991; Mori et al., 1992; Guthrie et

al., 1993; Shepherd, 1994; Cinelli et al., 1995). Odorant-induced activity involves distinct groups of glomeruli (Levetau and MacLeod, 1966; Stewart et al., 1979; Lancet et al., 1982; Guthrie et al., 1993; Shepherd, 1994), leading to the concept that odor information may be encoded by patterns of active glomeruli, which would determine the overall distribution of neuronal activity in the OB.

The discovery of a gene family encoding about 1000 different putative olfactory receptor (OR) proteins (Buck and Axel, 1991) has enabled a novel approach to olfactory coding. Individual members of this family are expressed in a small fraction of ORNs that are scattered in the olfactory epithelium (Ngai et al., 1993; Ressler et al., 1994b; Barth et al., 1996; Weth et al., 1996) but converge onto common glomeruli in the OB in rodents (Ressler et al., 1994a; Vassar et al., 1994; Mombaerts et al., 1996). Assuming that expression of an OR determines odorant selectivity, the odorant specificity of ORNs would be mapped on the glomeruli in the OB. The identity of an odorant would then be encoded by an activity pattern in the OB defined by a specific set of active glomeruli (Axel, 1995; Buck, 1996).

Direct analysis of such a coding strategy requires the monitoring of activity in the array of glomerular modules in response to substantial numbers of natural odorants, including both chemically similar and diverse molecules. In addition, to evaluate the performance of a combinatorial coding strategy, it is important to know the odorant-response spectra of individual glomerular modules and the degree of overlap between the responses of different modules. Whether mapping of afferents onto glomeruli is chemotopic, i.e., whether glomeruli are grouped physically according to their selectivity for defined molecular stimulus properties, is also unclear.

Here, we have directly addressed these questions using the zebrafish as a model system (Korsching et al., 1997). Compared to rodents, the zebrafish has ~10-fold fewer glomeruli (Baier and Korsching, 1994) and presumably also OR genes (Barth et al., 1996; Weth et al., 1996). Moreover, classes of ecologically relevant natural odorants have been identified for fishes, including AAs and bile acids (Caprio, 1988; Carr, 1988). Histologically, the organization of the OB in teleosts is not as clear cut as in mammals. Glomeruli often lack a prominent glial boundary and are revealed only by anterograde tracing of ORN axons (Oka et al., 1982; Riddle and Oakley, 1992; Baier and Korsching, 1994; Byrd and Brunjes, 1995). Nevertheless, the synaptic circuitry of the teleost OB is similar to that of all other vertebrate classes (Andres, 1970; Oka et al., 1982; Satou, 1992; Byrd and Brunjes, 1995).

In the present study, we have combined anterograde tracing of ORN axons with a  $\text{Ca}^{2+}$ -sensitive fluorescent dye and optical imaging in the OB. This technique allows us to selectively monitor the dynamic patterns of presynaptic activity in glomeruli induced by a large number of natural odorants in the same animal. The results obtained provide direct evidence that identity and concentration of odorants are encoded by combinatorial

\*Present address: Institut für Genetik der Universität zu Köln, D-50674 Köln, Federal Republic of Germany.

glomerular activity patterns in the OB. Mathematical analysis of activity patterns reveals a crude chemotopic organization of the array of glomerular modules and allows quantitative evaluation of the performance of combinatorial odorant coding.

## Results

### Optical Imaging of Presynaptic Activity in ORN Nerve Terminals

To investigate odorant coding, specifically at the input level in the OB, the entire population of ORNs was loaded with the  $\text{Ca}^{2+}$  indicator, Calcium Green-1 dextran. The dye was introduced into ORNs by injection into the nasal cavities in the presence of a low concentration of Triton X-100. This Triton treatment is known to selectively remove olfactory cilia and microvilli from ORNs without causing cells to degenerate and thereby allows efficient uptake of the dye. Cilia and microvilli then regenerate within a few days (Cancalon, 1983; Adamek et al., 1984). In zebrafish, we confirmed this by scanning electron microscopy: cilia and microvilli on ORNs are removed by Triton treatment and regenerate within 2 days (Figure 1). No regional bias was observed in ablation of cilia and microvilli. Within  $\sim 8$  hr after injection, the dye distributes throughout ORN axons. Labeling in the OB is uniform and specific for ORN axons and terminals, as concluded from comparison with preparations in which ORNs were labeled with lipophilic dyes (Baier and Korsching, 1994). Double labeling with Calcium Green-dextran and Dil in the same preparation further supports these observations ( $n = 3$  fish; not shown). No difference in responses to odorants was detected in fish examined immediately after regeneration of cilia and microvilli was complete (2 days after dye application) or at later stages (up to 5 days after application).

After a tracing and recovery period in vivo, an explant preparation of the olfactory system was used to optically image changes in  $[\text{Ca}^{2+}]$  in ORN axons in the OB, which was viewed ventrally. Electrical stimulation of the olfactory nerve elicits signals in the glomerular layer throughout the OB (Figures 2A and 2B;  $n = 13$  fish). Signals are abolished reversibly by  $\text{Ca}^{2+}$ -free medium ( $n = 5$ ) or addition of  $1 \mu\text{M}$  tetrodotoxin ( $n = 4$ ) (not shown). Recovery is complete after reintroducing  $\text{Ca}^{2+}$ , but only  $\sim 30\%$  after washing out tetrodotoxin for 1 hr, as expected from its high binding affinity. The signal is not continuous within the glomerular layer but consists of multiple foci of activity (Figure 2B). The anatomical correlates of these foci are neuropil structures that contain terminal arbors of afferent axons. No signals come from axon bundles coursing from the outer nerve layer into the glomerular layer (Figure 2C), presumably because  $\text{Ca}^{2+}$  channels are absent along ORN axons. Addition of  $100 \mu\text{M}$  2-amino-5-phosphonopivalic acid (APV) and  $20 \mu\text{M}$  6-cyano-7-nitroquinoxaline-2,3-dione (CNQX), antagonists of the putative ORN neurotransmitter glutamate (Shipley and Ennis, 1996), do not attenuate  $\text{Ca}^{2+}$  signals ( $n = 1$  fish; not shown). These results indicate that the signals observed reflect  $\text{Ca}^{2+}$  influx specifically in terminal axonal arbors of ORNs, presumably the presynaptic

$\text{Ca}^{2+}$  influx triggering transmitter release, as expected from the labeling procedure. This technique therefore allows us to selectively monitor presynaptic activity within glomerular modules.

Signals elicited by electrical stimulation are particularly prominent in a ventrolateral subregion of the OB, previously termed the "lateral chain" (Baier and Korsching, 1994) (Figure 2A). The reason for the difference in signal magnitude across the OB is unclear. In principle, signal intensity depends on the amount of  $\text{Ca}^{2+}$  influx, determined roughly by the density of voltage-gated  $\text{Ca}^{2+}$  channels, relative to a background, determined by the volume of labeled axons where no voltage-gated  $\text{Ca}^{2+}$  channels are present. Because  $\text{Ca}^{2+}$  influx is absent along axons but restricted to synaptic regions (Figures 2B and 2C), signal intensity should be highest in regions that are rich in dense glomerular neuropil. This is the case in the lateral chain (see below) and might therefore account for the prominent signals.

### Odorant-Induced Activity Patterns in the OB

To investigate olfactory coding, we initially screened different AAs and bile acids as olfactory stimuli. Signals induced by AAs were detected exclusively in the lateral chain, especially in the anterior and central parts (Figure 3A), while bile acids elicit signals in medial and posterior regions of the OB (not shown). These findings are substantiated by voltage-sensitive dye recordings (R. W. F., unpublished data). In other fish, field potential recordings also showed that AAs elicit strongest activity in the lateral OB, whereas activity elicited by bile acids is highest in the medial OB (Døving et al., 1980).

To examine olfactory coding in detail, we used L-AAs as stimuli that constitute a well-defined panel of natural odorants, comprising both chemically similar and diverse molecules (Caprio, 1988; Carr, 1988). Moreover, because AAs selectively activate the lateral chain where signals are prominent, a large number of odorants can be tested on the same preparation without the need for extensive signal averaging, and the majority of responding units can be imaged.

In a previous anatomical study (Baier and Korsching, 1994), the lateral chain was described as a stereotyped morphological structure of the zebrafish OB that is densely populated by ORN axons. It contains mainly neuropil that is not as clearly parcellated into glomeruli as many other regions of the OB. Since it has been suggested that the lateral chain might contain "hidden" glomeruli (Baier and Korsching, 1994), we have examined the substructure at a higher resolution by conventional and confocal microscopy. In preparations labeled with lipophilic tracers or Calcium Green-dextran, we find that afferent axons are initially fasciculated and terminate in circumscribed neuropil regions (Figure 2C; data not shown). These neuropil structures are the exclusive sites of  $\text{Ca}^{2+}$  influx into ORN axons (Figures 2B and 2C) and respond individually to odorants (Figure 3B). Thus, they constitute functional and anatomical units containing terminal arborizations of converging ORN axons, and would therefore fulfill the criteria for glomeruli. However, we will conservatively refer to these units as "glomerular modules" because, compared to glomeruli

in other regions of the OB, they are smaller, often less distinctly delineated, and more densely packed. The total number of glomerular modules in the lateral chain is estimated to be  $\sim 120$  (see Experimental Procedures).

Like electrical stimulation, AA stimuli induce discrete foci of activity in the lateral chain, the anatomical correlates of which are individual glomerular modules (Figure 3B). The odorant-activated glomerular modules are a subset of the total number of modules that can be activated by electrical stimulation of the olfactory nerve (Figure 2B). Individual glomerular modules respond independently to odorants (Figure 3B). Rarely, small negative signals are observed. Activity patterns are highly

reproducible upon repeated application of the same AA (Figures 3C and 3D). The correlation (see below and Table 1) between patterns elicited in repeated stimulations is usually  $>0.96$ .

The time course of the signal in each glomerular module consists of an initial increase, a peak, and a decline of signal intensity (Figure 3D). No complex time courses, such as biphasic or oscillatory responses, were observed. In some cases, such as that shown in Figure 3D, timing differences of up to 0.5–1 s in the response onset are apparent between glomerular modules, possibly reflecting different response latencies of ORN types (Ivanova and Caprio, 1993; Firestein et al., 1993).

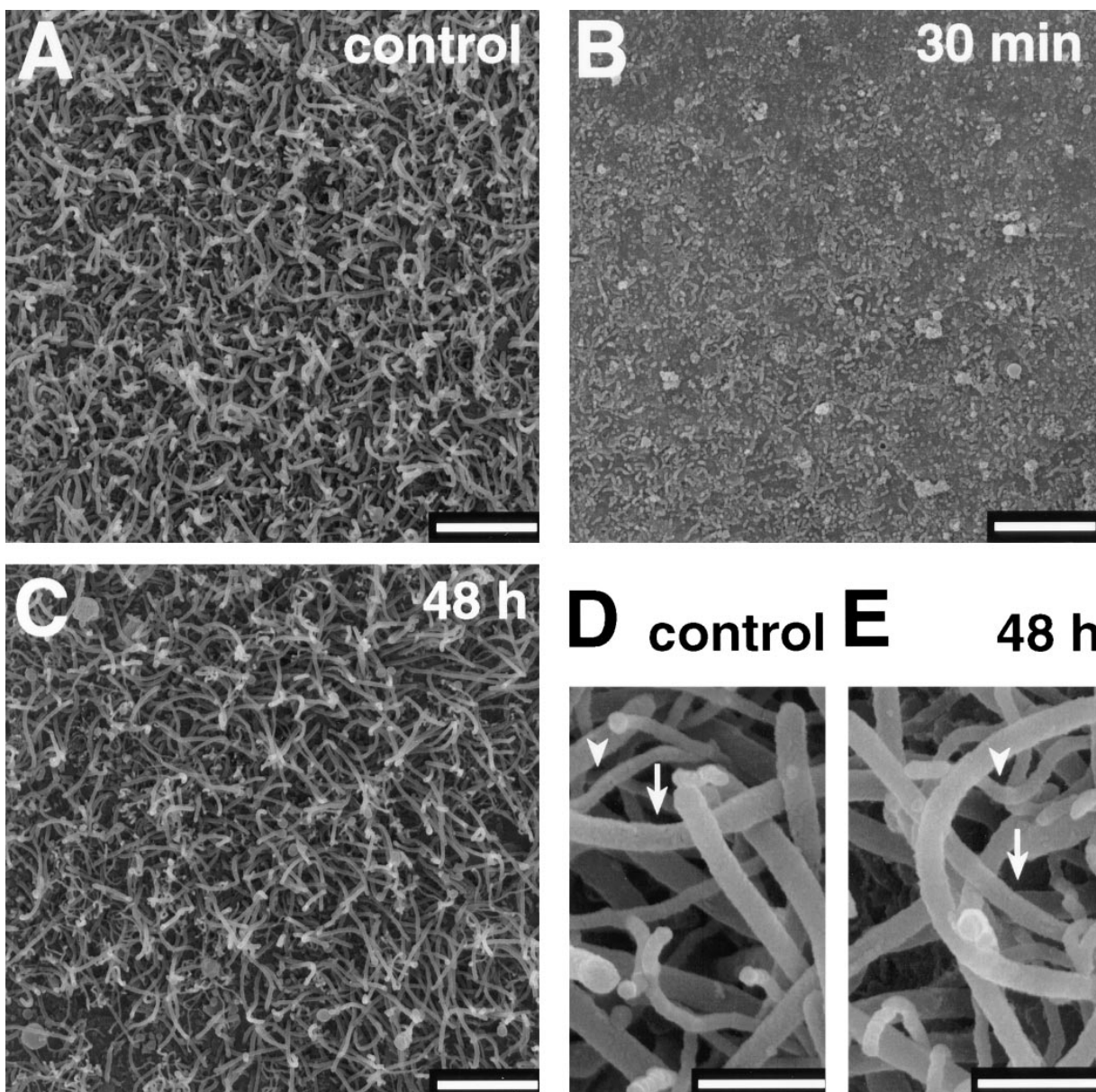
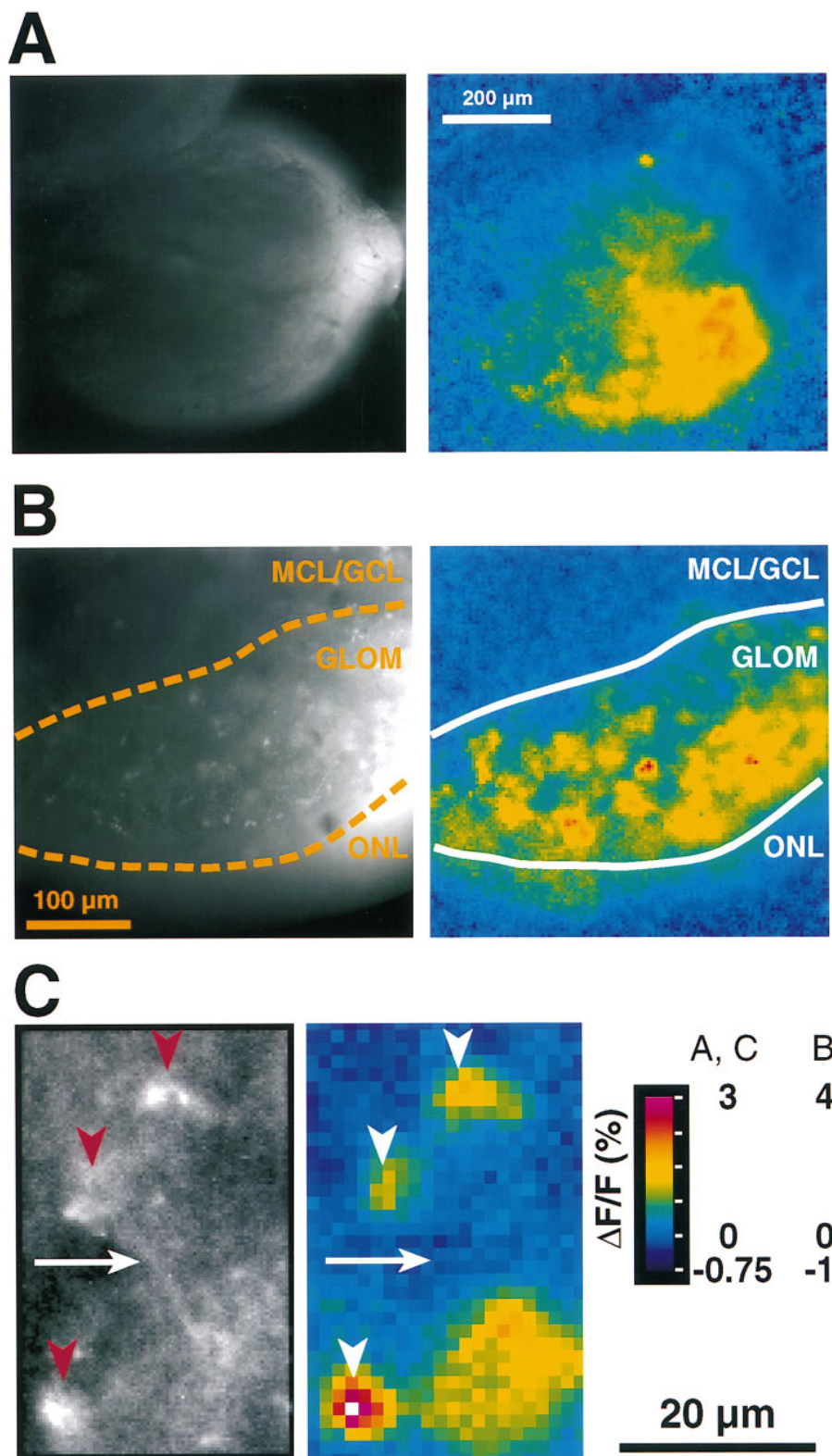


Figure 1. Ablation and Regeneration of Olfactory Cilia and Microvilli

Images show scanning electron micrographs of the sensory surface of olfactory lamellae of an untreated epithelium (A) and epithelia 30 min (B) and 48 hr (C) after application of Triton X-100 and Calcium Green-dextran. Higher magnification shows olfactory cilia (arrows) and microvilli (arrowheads) in an untreated epithelium (D) and an epithelium 48 hr after Triton/Calcium Green-dextran application (E). Olfactory cilia and microvilli are uniformly removed by Triton treatment and regenerate within 48 hr. Scale bars, 6  $\mu\text{m}$  (A–C); 1  $\mu\text{m}$ , (D and E).



We then compared patterns of glomerular activity induced by AAs in the central and anterior part of the lateral chain, where the majority of AA-sensitive glomerular modules are found (Figure 3A). Each of 18 different AAs tested induced a unique glomerular pattern of activity (Figure 4A). Individual glomerular modules are usually activated by multiple AAs and participate in different activity patterns (Figures 4A and 4B). Hence, the identity of a stimulus is encoded unambiguously by a pattern of active glomerular modules in a combinatorial fashion. The average fraction of modules activated by AAs (those of Figure 4A, except Pro and D-Ala; 10  $\mu$ M) is 33% (range, 11% for Asp to 62% for Met).

Most glomerular modules have unique odorant selectivities (Figure 4B); in about 80% of the cases, odorant-response profiles for different modules are correlated by  $<0.5$  (for AAs at 10  $\mu$ M). Individual glomerular modules usually exhibit broad and complex odorant-response profiles (Figure 4B). Glomerular modules with similar response profiles are often located close to each other and sometimes form clusters, but neighboring modules can also display very different response profiles (Figure 4; see also Figures 6C and 6D). In some cases, the odorant-response profile of a glomerular module is obviously correlated with the chemical properties of the stimuli. For example, some glomerular modules respond preferentially to basic AAs, to neutral AAs, and to a subgroup of neutral AAs (Leu, Ile, Val, and Met) (modules 1–3 in Figure 4B). Often, however, no obvious correlation of the response profile with the chemical properties of the odorants is apparent. D-Ala and Pro elicit little activity. This observation is consistent with electroolfactogram recordings and shows that the L-configuration and a free  $\alpha$ -amino group are necessary to efficiently activate AA receptors (Caprio and Byrd, 1984; Michel and Lubomudrov, 1995).

General features of glomerular activity patterns are constant across individuals, as revealed by comparison of patterns of active modules, induced by the panel of 18 AAs, in different animals. The relative distribution of active glomerular modules is similar for a given AA, and systematic differences in patterns obtained with different AAs are apparent across animals. In each animal, characteristic groups of active glomerular modules are always located at similar relative positions (Figures 4A, 4C, and 4D). For example, clusters of modules responding preferentially to basic AAs, to neutral AAs, and to a subgroup of neutral AAs (Val, Ile, Leu, and Met), are always located anteriorly, centrally, and posteriorly, respectively (Figures 4A, 4C, and 4D). Furthermore, signals induced by acidic AAs are always weak, and D-Ala and Pro elicit even less signal. On the level of single glomerular modules, however, activity patterns induced by the same AA in different animals are not found to be identical. This may at least in part be due to slight differences in the orientation of preparations.

With increasing concentration of an AA, the number

of active glomerular modules also increases (Figure 5A), possibly reflecting the activation of ORs with progressively higher  $K_D$  values. Concentration-response functions for individual glomerular modules can have various shapes and thresholds (Figure 5B), indicating that different glomerular modules can respond differently to a given odorant. The lowest thresholds are between 10 nM and 100 nM (for Met), while the highest thresholds are between 100 nM and 1  $\mu$ M, consistent with electroolfactogram recordings (Michel and Lubomudrov, 1995).

It is possible that combinatorial odorant coding depends on the concentration of odorants. For example, at lower concentrations, individual AA-induced activity patterns could be separated more clearly because they would exhibit less overlap, or they may be more similar for some stimuli if these would activate only a small, common set of glomerular modules around threshold. Furthermore, the activity pattern induced by an AA at a given concentration might be identical to the pattern induced by another AA at another concentration. To explore these possibilities, we examined glomerular activity patterns induced by 16 AAs (those of Figure 4A, except D-Ala and Pro) at three concentrations in the same preparation (1  $\mu$ M, 10  $\mu$ M, and 100  $\mu$ M;  $n = 5$  fish). Each activity pattern was found to be unique (not shown), indicating that odorants are encoded in a combinatorial fashion over a broad concentration range, and that glomerular activity patterns could encode both stimulus identity and concentration.

#### Quantitative Analysis of Odorant-Induced Activity Patterns

Visual inspection of glomerular activity patterns induced by different AAs gives the impression that the similarity of patterns is highest for AAs that are chemically closely related. Clear differences are apparent between patterns elicited by different chemical classes of AAs such as neutral, acidic, and basic AAs (Figure 4A). Moreover, glomerular activity patterns appear to contain substructures such as clusters of glomerular modules with similar response profiles.

To quantitatively analyze these features of glomerular activity patterns by multivariate statistics (Bieber and Smith, 1986), active glomerular modules were mapped and the odorant-response profiles were determined to obtain a matrix of stimuli versus modules (see example in Figure 4B). The total number of identifiable glomerular modules activated by 16 AAs (those of Figure 4A, except D-Ala and Pro) was  $61 \pm 4$  (at 1  $\mu$ M),  $86 \pm 8$  (at 10  $\mu$ M), and  $95 \pm 12$  (at 100  $\mu$ M; means  $\pm$  SEM). From this matrix, the Pearson product moment correlation matrix was calculated (Table 1), which is a quantitative measure for the similarity between patterns. Furthermore, hierarchical cluster analysis was performed (Figure 6A), which links stimuli according to the similarities of the corresponding activity patterns (Bieber and Smith, 1986). These analyses reveal groups of stimuli whose patterns

(C) ORN axon labeling and  $\text{Ca}^{2+}$  signals within the glomerular layer of the subregion responsive to AAs. Note that focal signals originate exclusively from glomerular modules (arrowheads) but not from axon bundles (arrow). The signal in the lower right comes from a glomerular module that is somewhat out of focus and appears less clearly delineated. In (A–C), signals were evoked by a 32 Hz pulse train delivered to the entire olfactory nerve through a suction electrode. Throughout, anterior is to the right and lateral is to the bottom.



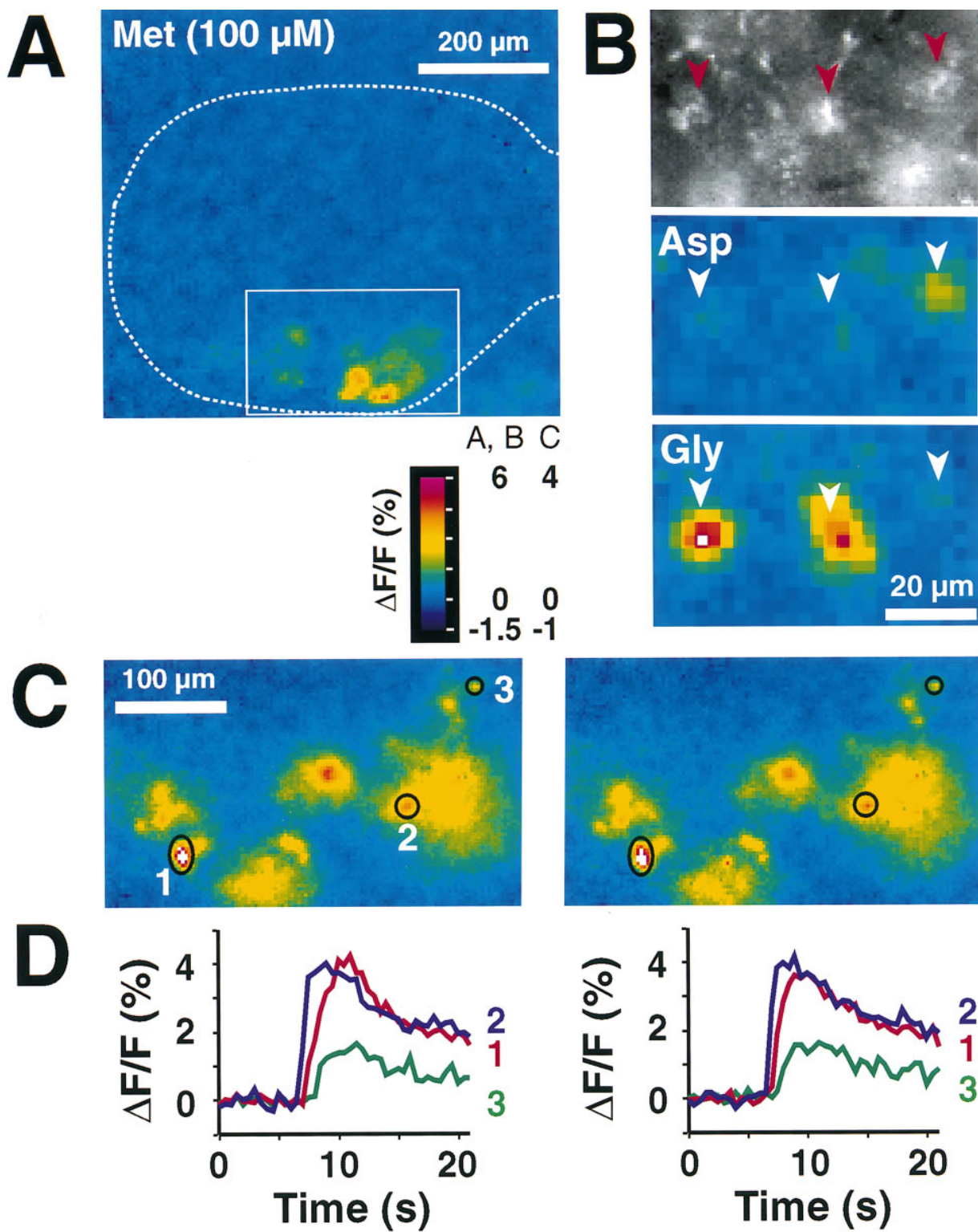


Figure 3.  $\text{Ca}^{2+}$  Signals in the OB Elicited by AAs

(A)  $\text{Ca}^{2+}$  signals in the entire OB induced by 100  $\mu$ M Met, which is the AA that induces the most widespread distribution of glomerular activity within the OB. The view of the OB is similar to Figure 2A, and the outline of the OB is indicated by the dashed line. Note that signals are confined to a ventrolateral subregion. Responses to other AAs consist of different patterns but are confined to the same subregion of the OB. The box approximates the ventrolateral subregion that is shown in Figures 3C, 4A, 4B, 4C, 4D, 5A, 6C, and 6D.

(B) ORN axon labeling within the glomerular layer of the AA-responsive subregion of the OB, and signals induced by two different AAs (1  $\mu$ M) in the same view showing that AAs differentially activate glomerular modules.

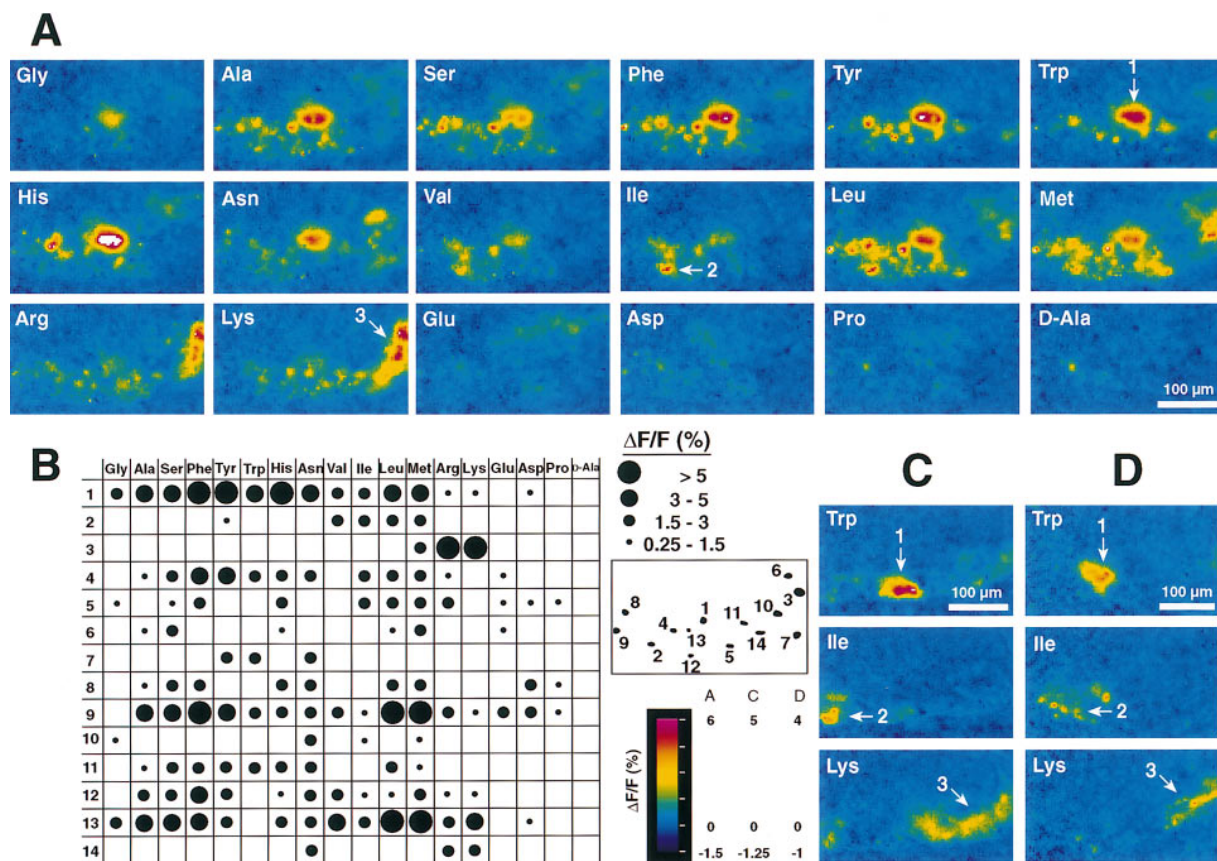


Figure 4. Glomerular Activity Patterns in the OB Induced by AAs  
(A) Glomerular activity patterns induced by 18 AAs (10  $\mu$ M) in the AA-responsive subregion of the OB. Note that each stimulus induces a unique glomerular activity pattern. Arrows depict characteristic clusters of glomerular modules responding preferentially to all neutral AAs (1); to Val, Ile, Leu, and Met (2); and to basic AAs (3).  
(B) Odorant-response profiles of a subset of glomerular modules from the experiment shown in (A). Positions of these glomerular modules are depicted by the drawing. 1–3 are from the clusters depicted by arrows 1–3, respectively.  
(C and D) Responses to three AAs (10  $\mu$ M) in the AA-responsive subregion in two other fish, demonstrating similarities of activity patterns across individuals. Arrows depict groups of foci corresponding to those in (A). Throughout, anterior is to the right and lateral is to the bottom.

show a high degree of similarity. These groups comprise AAs with common molecular properties, indicating that similarity of glomerular activity patterns is correlated with similarities in certain molecular properties of odorant stimuli.

To further examine the relation between molecular features of stimuli and inherent features of activity patterns, we performed a factor analysis. This mathematical technique expresses the patterns induced by the panel of stimuli as a combination of a smaller number of “principal” patterns induced by hypothetical “principal” stimuli (factors) (Rummel, 1970; Bieber and Smith, 1986). Factor analysis extracts four factors, indicating that AA stimuli contain at least four principal molecular features that are reflected in glomerular activity patterns. The

large loadings ( $>0.5$ ) on each of the factors are associated with groups of stimuli identical to the groups established by hierarchical cluster analysis (Figures 6B and 6C). These groups comprise AAs with common molecular features: (1) neutral AAs with short aliphatic residues with or without an aromatic or heterocyclic extension (Ala, Ser, Phe, Tyr, Trp, and His), (2) basic AAs (Arg and Lys), (3) neutral AAs with long nonpolar aliphatic residues (Val, Ile, Leu, and Met), and (4) acidic AAs (Glu and Asp). Previously, similar groups of AAs were established in cross-adaptation assays and were termed (1) short-chain neutral, (2) basic, (3) long-chain neutral, and (4) acidic AAs (Caprio and Byrd, 1984; Caprio, 1988). The common molecular properties within these groups allow the inference of the principal molecular properties

(C) Activity patterns induced in the AA-responsive subregion of the OB by repeated application of 100  $\mu$ M Met. Preparation and focal plane are different from (A).  
(D) Time course of signals in three selected regions in (C). Graphs correspond to the activity patterns above (C). Throughout, anterior is to the right and lateral is to the bottom.

Table 1. Similarities of Glomerular Activity Patterns Induced by AAs

	Gly	Ala	Ser	Phe	Tyr	Trp	His	Asn	Val	Ile	Leu	Met	Arg	Lys	Glu	Asp
Gly																
Ala	0.47															
Ser	0.36	0.67														
Phe	0.56	0.62	0.53													
Tyr	0.50	0.60	0.44	0.81												
Trp	0.54	0.52	0.42	0.73	0.82											
His	0.42	0.63	0.56	0.70	0.64	0.62										
Asn	0.37	0.50	0.39	0.55	0.54	0.57	0.52									
Val	0.44	0.41	0.27	0.36	0.42	0.35	0.29	0.30								
Ile	0.37	0.36	0.25	0.32	0.37	0.32	0.27	0.27	0.75							
Leu	0.46	0.49	0.46	0.52	0.45	0.36	0.38	0.37	0.57	0.60						
Met	0.25	0.31	0.34	0.29	0.23	0.17	0.26	0.20	0.39	0.37	0.60					
Arg	-0.01	-0.13	-0.01	-0.05	-0.07	-0.03	-0.07	-0.04	0.02	-0.01	0.12	0.33				
Lys	-0.03	-0.17	0.00	-0.12	-0.14	-0.06	-0.12	-0.06	-0.12	-0.14	0.00	0.20	0.69			
Glu	-0.01	0.09	0.24	-0.02	-0.09	-0.02	0.15	-0.01	-0.04	-0.05	0.02	-0.01	0.00	-0.02		
Asp	0.07	0.15	0.26	0.22	0.15	0.19	0.24	0.23	0.21	0.22	0.22	0.12	0.08	-0.03	0.28	

Pearson product moment correlation matrix depicting similarities between activity patterns induced by AAs (10  $\mu$ M; n = 6 preparations). Similar results were obtained for stimuli at 1  $\mu$ M (n = 5) or 100  $\mu$ M (n = 6). Values  $\geq 0.6$  are shown in bold; values  $\geq 0.7$  are bold and underlined; values  $< 0$  are in italics. Note that the Table is mirror symmetric about the diagonal.

of AAs that are reflected in distinct features of glomerular activity patterns (Rummel, 1970; Bieber and Smith, 1986).

Because the communality is not close to unity for any of the stimuli (Table 2), the extracted principal molecular features cannot account for all of the properties of the actual stimuli. Several stimuli have moderate loadings on multiple factors, indicating that they combine multiple principal molecular features. Within the neutral AAs, Gly and Asn have particularly low communalities (Table 2) and are not tightly linked to a particular group by hierarchical clustering (Figure 6A). For Gly, this is conceivably because it lacks a side chain, while Asn has chemical properties that partially conflict with the principal molecular features extracted. The group of "short-chain neutral" AAs seems to separate into subgroups comprising AAs with (Phe, Tyr, Trp, and His) and without (Ala and Ser) an aromatic or heterocyclic extension. The group of acidic AAs is only loosely linked by hierarchical clustering. Moreover, factor analysis tends to separate the factor associated with the acidic AAs into two factors, if it is set to extract a fixed number of five factors in total (not shown). This is remarkable because Glu and Asp differ only by one carbon atom in chain length.

The factors extracted are to be understood as hypothetical stimuli with "pure" principal molecular features (Rummel, 1970; Bieber and Smith, 1986). To examine how principal molecular features would be represented within the array of glomerular modules, we reconstructed the (hypothetical) activity patterns associated with each of the factors. Each factor is represented by a distinct group of active glomerular modules (Figures 6C and 6D). These groups are readily recognized in the original activity patterns and include the characteristic clusters noticed by visual inspection (compare Figure 4A with Figures 6C and 6D). Importantly, the groups of glomerular modules representing each factor tend to be located within confined regions. Factors 1–3 are represented by glomerular modules concentrated in central, anterior, and posterior regions, respectively (Figures 6C and 6D). Glomerular modules associated with factor 4 ("acidic") are found in two regions located anteriorly and posteriorly. When factor 4 is subdivided into two factors by extracting a fixed number of five factors in total, each of these regions is associated with a different factor (not shown).

The results reported (Figure 6; Tables 1 and 2) were obtained with AAs at 10  $\mu$ M (n = 6 fish), which is within the relevant physiological range, as concluded from the environmental concentration of AAs (Carr, 1988), electroolfactogram recordings (Michel and Lubomudrov, 1995), and behavioral studies (e.g., Zippel et al., 1993). The same analyses were also performed for AAs at 1  $\mu$ M (n = 5), which is only slightly above threshold for some AAs, and at 100  $\mu$ M (n = 6). The results obtained are similar to those obtained at 10  $\mu$ M, and the same regions associated with factors are found (not shown), indicating that the same inherent features of activity patterns are present and the same principles of odorant coding operate over a wide range of concentrations.

The finding that individual factors are represented by glomerular modules concentrated in confined regions indicates that the principal molecular properties of stimuli are mapped onto the array of glomerular modules.



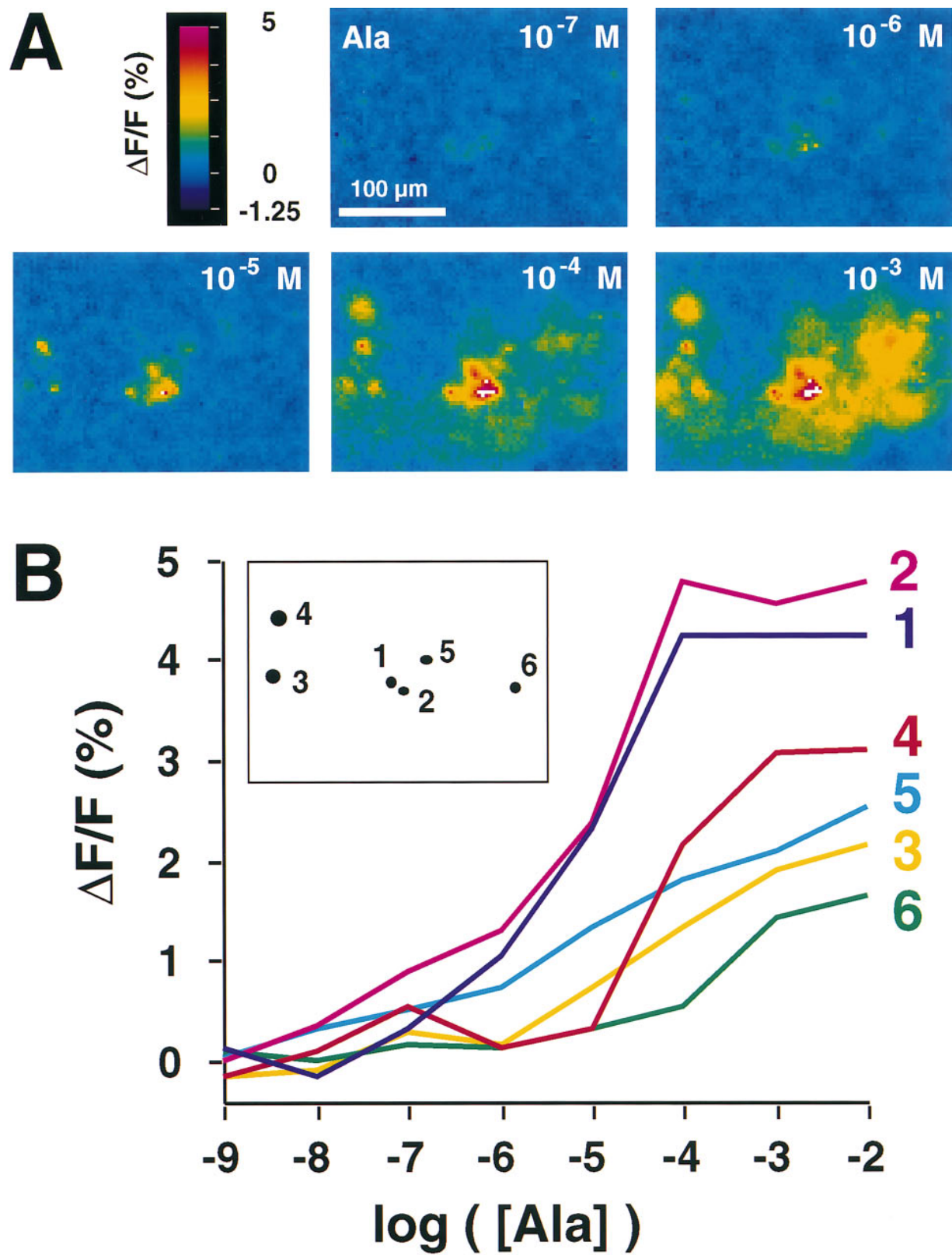
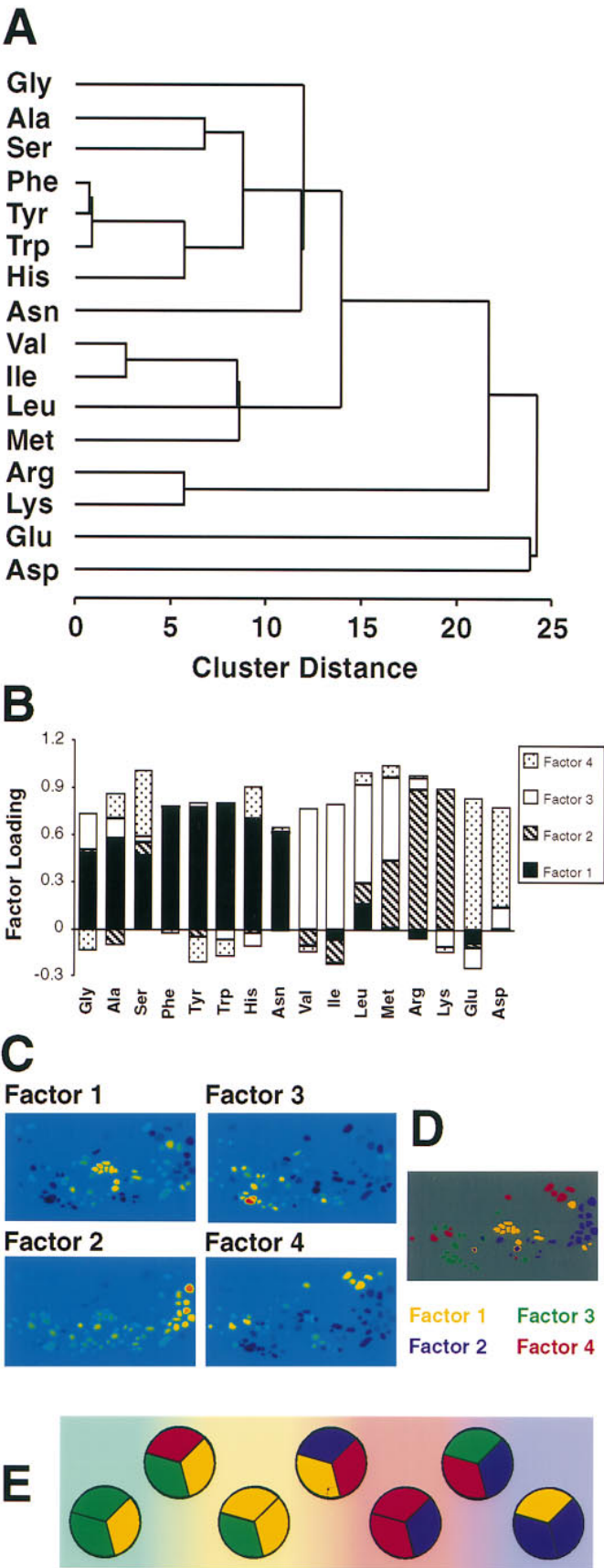


Figure 5. Dose-Response Characteristics of Odorant-Induced Activity Patterns

(A) Responses to five concentrations of Ala. Anterior is to the right and lateral is to the bottom.

(B) Concentration-response curves for individual glomerular modules in (A). The positions of the respective glomerular modules are depicted in the drawing (inset).



**Figure 6. Multivariate Analysis of Odorant-Induced Activity Patterns**

(A) Hierarchical cluster analysis depicting relationship between 16 AAs (10  $\mu$ M) based on the similarity of the associated activity patterns (single linkage). Similarity is expressed by cluster distance, with small distance indicating high similarity (Bieber and Smith, 1986). Computed from the same data as Table 1 ( $n = 6$  preparations).

(B) Factor analysis results (oblique solution reference structure) after rotation and transformation (principal components; orthotransvarimax), computed from the same data as (A) and Table 1. Similar results were also obtained for AAs at 1  $\mu$ M ( $n = 5$  preparations) and 100  $\mu$ M ( $n = 6$ ). Factor loadings are a measure for the contribution of each factor to the glomerular activity patterns induced by AAs (Rummel, 1970; Bieber and Smith, 1986). Unrotated factors and communality estimates are shown in Table 2.

(C) Reconstruction of the hypothetical activity patterns corresponding to the four factors for the experiment shown in Figure 4A. The region and the color code are identical to that in Figure 4A.

(D) Comparison of glomerular activity patterns representing factors. Glomerular modules that are strongly activated in (C) ( $\Delta F/F > 1.8\%$ ) are color coded for each factor and superimposed. Note that strongly activated glomerular modules are concentrated in regions specific for each factor. The relative positions of these regions are constant across individuals.

(E) Simplified model summarizing olfactory coding by combinatorial and chemotopic glomerular activity patterns. Circles depict glomerular modules, and colors indicate responsiveness to principal molecular features of odorants. Glomerular modules exhibit broad and complex odorant tuning indicated by multiple colors. An odorant stimulus would induce a complex pattern of active glomerular modules according to its molecular properties. The fine-grained structure of this pattern encodes the identity of the odorant stimulus. In addition, glomerular modules responding to particular molecular properties tend to be located within confined regions of the glomerular array. This organization establishes a coarse chemotopic map, indicated by background colors. General chemical features of odorants are therefore represented by the global distribution of activity. Note that this model is oversimplified because the response profiles of glomerular modules also contain unique components that cannot be fully accounted for by a combination of principal molecular properties.

Table 2. Factor Analysis Results

	Factor 1	Factor 2	Factor 3	Factor 4	SMC	Final est.
Gly	0.67	0.02	0.06	-0.19	0.439	0.491
Ala	0.79	-0.14	-0.08	0.07	0.636	0.651
Ser	0.68	0.02	-0.28	0.28	0.555	0.617
Phe	0.84	-0.15	-0.18	-0.18	0.756	0.799
Tyr	0.82	-0.19	-0.10	-0.28	0.788	0.805
Trp	0.78	-0.18	-0.22	-0.27	0.729	0.752
His	0.76	-0.18	-0.30	0.04	0.602	0.705
Asn	0.67	-0.12	-0.18	-0.10	0.414	0.501
Val	0.63	0.22	0.56	0.10	0.623	0.767
Ile	0.59	0.21	0.61	0.15	0.621	0.786
Leu	0.72	0.35	0.28	0.10	0.631	0.726
Met	0.47	0.60	0.14	0.06	0.459	0.602
Arg	-0.02	0.83	-0.32	-0.15	0.532	0.816
Lys	-0.12	0.75	-0.43	-0.23	0.516	0.813
Glu	0.06	-0.01	-0.36	0.76	0.201	0.703
Asp	0.32	0.10	-0.14	0.59	0.222	0.480

Unrotated factor analysis results for data pooled from six preparations (AAs at 10  $\mu$ M). Results after rotation-transformation (oblique solution reference structure) are displayed in Figure 6B. The last two columns give the communality estimate. Squared multiple correlation (SMC) refers to the unrotated results; the final estimate refers to the results after rotation-transformation (Figure 6B).

This mapping is constant across individuals because the relative positions of the regions associated with factors are the same for each individual (not shown; but see Figures 4C and 4D). The glomerular array therefore exhibits a coarse chemotopic organization in addition to its combinatorial properties.

## Discussion

### Optical Imaging of Activity in Glomerular Modules

We have devised a method that combines *in vivo* axonal tracing and subsequent optical imaging in an explant preparation to monitor presynaptic activity in glomerular modules of the zebrafish OB. For analysis of olfactory coding, we concentrated on AAs, which selectively activate a morphologically defined ventrolateral subregion of the OB, the lateral chain (Baier and Korsching, 1994). This subregion appears to be the only region of the OB that responds to AAs, although it cannot be ruled out that weak signals in dorsal regions were not detected because the OB was viewed ventrally.

The exclusive localization of AA responses to the lateral chain implies a functional specialization of this OB subregion. Indications for functional specializations of OB subregions have also been reported for other fish species (Døving et al., 1980; Satou, 1992) and for mammals (Imamura et al., 1992; Mori et al., 1992; Katoh et al., 1993). In rodents, ORs are expressed in the olfactory epithelium within broad zones that project to corresponding regions of the OB (Ressler et al., 1994b). Similar expression domains, though less clearly delineated, have recently been found in the zebrafish olfactory epithelium as well (Weth et al., 1996). It will now be interesting to see whether there is a correlation between functionally specialized subregions of the OB and OR expression domains.

We imaged activity in an anterior-central region of the

lateral chain that receives the majority of afferent axons and contains most of the structures responding to AAs. Within the imaged region, ORN axons are organized into  $\sim 120$  glomerular modules. These modules were not described in a previous study of the pattern of glomeruli in the zebrafish OB (Baier and Korsching, 1994), presumably because the OB was viewed at a lower magnification, because two-dimensional projections of relatively thick stacks of optical sections were examined, and because glomerular modules are smaller and less clear cut in appearance than glomeruli in other OB regions. Labeling of glomerular modules by anterograde tracers is intense compared with most glomeruli outside the lateral chain, suggesting that the density of presynaptic structures is high. This is consistent with the finding that electrically induced  $\text{Ca}^{2+}$  signals are more prominent in these glomerular modules than in most other areas of the OB.

The lateral chain is innervated by a substantial fraction of ORN axons, which we estimate as 20%–60%, based on the labeling intensity with Calcium Green-dextran or lipophilic tracers. Given that the zebrafish olfactory epithelium contains  $\sim 40,000$  ORNs (Barth et al., 1996; Korsching et al., 1997), the number of axons converging onto each glomerular module would be on the order of 100. Compared to glomeruli in other OB regions, glomerular modules are smaller in size and their appearance is not as clear cut, but they clearly constitute anatomical and functional units. Glomerular modules thus exhibit the characteristics of glomeruli, but it is also possible that some are substructures of larger entities such as fused glomeruli, although there is little indication for this possibility. A great variability in size and appearance of glomeruli is also common in other regions of the zebrafish OB and in other fish species (Oka et al., 1982; Riddle and Oakley, 1992; Baier and Korsching, 1994).

Glomerular modules are the exclusive sites of  $\text{Ca}^{2+}$  influx into ORN axons (Figures 2B and 2C) and respond independently to odorants (Figure 3B). These results directly demonstrate that glomerular modules act as functional units and are the basic elements underlying activity patterns in the OB. This is consistent with responses of glomeruli in mammals (Levetau and MacLeod, 1966; Lancet et al., 1982; Guthrie et al., 1993; Shepherd, 1994), and further indicates that glomerular modules in zebrafish constitute functional units comparable to glomeruli in other vertebrate species.

### Odorant Coding by Glomerular Activity Patterns

Each AA stimulus induces a unique, complex pattern of active glomerular modules, providing direct evidence that odorant identity is encoded by the array of glomerular modules in a combinatorial fashion. The combinatorial nature of this coding strategy allows encoding of a large number of different odors, far exceeding the number of modules and OR genes. Furthermore, activity patterns encode information about odorant concentration since different glomerular activity patterns are also elicited by different odorant concentrations. With increasing concentration, odorants recruit increasing numbers of glomerular modules, but the basic features

of activity patterns are retained (at least in the micromolar range), indicating that information about odorant concentration is encoded by glomerular modules that receive input from ORs with different affinities.

Across individuals, several characteristic features of glomerular activity patterns are constant. These features include the relative distribution of activity and characteristic groups of glomerular modules defined by their relative position and odorant-response profiles. Variation in the orientation of preparations and in the fine morphology does not allow a detailed module-by-module comparison of activity patterns across individuals. It is therefore not clear whether the functional constancy extends to the level of single glomerular modules. However, the high degree of functional constancy parallels the general morphological stereotypy of the glomerular pattern (Baier and Korsching, 1994) and implies substantial hardwiring in the functional organization of the primary olfactory projection (Mombaerts et al., 1996). Studying the maturation of glomerular activity patterns may provide further insights into the mechanisms that establish the functional array of glomerular modules during development.

Previous experimental approaches have shown that odorants induce differential distributions of activity within the OB, which agree with our results (Adrian, 1953; Moulton, 1967; Stewart et al., 1979; Kauer, 1991; Mori et al., 1992; Cinelli et al., 1995). These approaches have detected activity predominantly in mitral cells and OB interneurons but did not allow resolution of activity at the level of glomeruli. Other studies have demonstrated that single glomeruli function independently and respond differentially to odorants, which is also consistent with our results (Levetau and MacLeod, 1966; Stewart et al., 1979; Lancet et al., 1982; Guthrie et al., 1993). However, the techniques used had strong restrictions on either the number of stimuli or the number of glomeruli that could be examined. We have now clearly defined the response properties of many glomerular modules simultaneously at the input level. Our results therefore provide direct insight into how information is encoded in the combinatorial response of the ensemble of glomerular modules. Since general response properties of glomerular modules in the lateral chain are similar to those of mammalian glomeruli, the combinatorial coding strategy characterized here is likely to be important for all vertebrates.

AAs provide a class of natural odorants containing both chemically similar and diverse odorants. Although we find that the similarity of glomerular activity patterns is correlated with molecular properties of stimuli, even very similar pairs such as Ala and Ser, Leu and Ile, or Arg and Lys induce unique activity patterns. Behavioral studies have shown that fish can be conditioned to discriminate between such similar AAs (Zippel et al., 1993). This suggests that information about odorant identity and concentration encoded within complex glomerular activity patterns can indeed be extracted in further steps of information processing and used to generate behavioral responses.

#### Cellular and Molecular Implications of Glomerular Activity Patterns

In rodents, axons of ORNs that express the same OR converge onto distinct glomeruli in the OB, leading to

a model in which each glomerulus is activated by a particular set of odorants such that the identity of a stimulus would then be encoded in a combinatorial activity pattern (Ressler et al., 1994a; Vassar et al., 1994; Axel, 1995; Buck, 1996; Mombaerts et al., 1996). Our experiments are a functional test for this model; indeed, we find that odorants are encoded by specific combinatorial patterns of active glomerular modules.

Several features of odorant-induced glomerular activity patterns corroborate predictions from the above model. First, individual glomerular modules have broad response spectra. If each glomerular module received input from only one population or a few populations of ORNs, as suggested by molecular data (Axel, 1995; Buck, 1996), individual ORNs would also be expected to be broadly tuned, which has in fact been shown (Revial et al., 1982; Firestein et al., 1993; Ivanova and Caprio, 1993; Kang and Caprio, 1995). Second, activity patterns include characteristic clusters of glomerular modules with similar response spectra. In mice, clusters of glomeruli have been described that receive input from one OR or from a few ORs of the same subfamily, which are thought to have similar odorant selectivity (Ressler et al., 1994a). In theory, such connectivity could account for the characteristic clusters of glomerular modules in zebrafish. Third, odorant-specific glomerular activity patterns are highly stereotyped across individuals. This is consistent with the constant positions of glomeruli specified by input from defined ORs (Ressler et al., 1994a; Vassar et al., 1994; Mombaerts et al., 1996). Thus, a convergence principle similar to that demonstrated in rodents may also underlie the functional organization of the array of glomerular modules in zebrafish. However, direct evidence is lacking because it has not yet been shown whether ORNs expressing a given OR converge onto single glomeruli in vertebrates other than rodents.

Although it is likely that defined populations of ORNs converge onto specific glomerular modules (see also next section), there are several possibilities for how glomerular modules may be connected to the expression of ORs in the olfactory epithelium. First, since ORNs express a small number of ORs, possibly only one (Ngai et al., 1993; Chess et al., 1994; Ressler et al., 1994b; Barth et al., 1996; Weth et al., 1996), each glomerular module might receive input from only one type of ORN expressing only one OR. In rodents, several experimental results favor this possibility (Axel, 1995; Buck, 1996). Second, ORNs might express a combination of ORs, which has been suggested because ORNs can respond to odorants with both excitation and inhibition. This has been observed frequently in fish (Ivanova and Caprio, 1993; Kang and Caprio, 1995) but also in mammals (Revial et al., 1982; Getchell, 1986). Third, a given glomerular module might be innervated by multiple types of ORNs expressing different (combinations of) ORs. For example, axons expressing different markers converge onto common glomeruli in mice, but it is unknown whether these markers are associated with differential expression of ORs (Treloar et al., 1996).

If a given glomerular module received input from only one OR, the broad and complex odorant-response profiles should directly reflect the odorant selectivity of the underlying OR. Complex tuning of ORs could be brought about by multiple sites for odorant-OR interaction,



involving both binding sites that activate the receptor and binding sites or steric barriers that inhibit receptor activation. Such a view would be consistent with structural models of ORs (Shepherd, 1994) and with ligand-receptor interactions at related seven-transmembrane receptors (Strader et al., 1994). Unraveling the connection between OR expression and glomerular modules might therefore provide immediate insight into ligand-OR interactions, which are currently not well understood.

### The Internal Structure of Glomerular Activity Patterns

In principle, glomerular modules could be arranged randomly, or they could be organized according to selectivity for certain molecular stimulus properties. To investigate these possibilities, we determined systematic relationships between the molecular structure of odorants and features of glomerular activity patterns by multivariate analysis.

Since the response profiles of most glomerular modules are broad and do not correlate with obvious molecular features of stimuli, little information about the chemical structure of a stimulus can be obtained from the response of a single glomerular module. However, stimuli inducing similar glomerular activity patterns have common principal molecular features. General information about the structure of odorant molecules is therefore contained in the overall pattern of active glomerular modules. At least four principal molecular features represented within glomerular activity patterns can be distinguished (factors 1–4), each associated with a group of AAs (Figures 6A and 6B).

Virtually the same groups of AAs were found in competitive binding assays with olfactory cilia (Rhein and Cagan, 1983) and in cross-adaptation studies of electroolfactogram responses in fish (Caprio and Byrd, 1984; Caprio, 1988). These studies indicate that AAs within a group are likely to activate common types of ORs. Given that the same AAs also activate common glomerular modules, at least part of the glomerular odorant specificity appears to be determined by convergence of ORNs expressing common ORs.

The principal molecular features represented by factors appear to play an important role in olfactory recognition, both on the level of OR-ligand binding and on the level of patterning the glomerular response. Reconstruction of the hypothetical representations of the factors by glomerular activity patterns reveals that each factor is represented by groups of glomerular modules that are regionally concentrated. Thus, information about defined principal stimulus properties that is likely to be distinguished already on the level of OR-ligand binding is segregated within the array of glomerular modules. The primary olfactory projection therefore systematically maps information about molecular structure onto the OB, so that the array of glomerular modules exhibits a coarse chemotopic organization.

Our results have revealed two levels of organization in olfactory coding by the array of glomerular modules: single modules display complex odorant tuning, whereas the overall array exhibits a coarse chemotopic organization. As a consequence, the precise identity of

an odorant is encoded in the fine-grained structure of the glomerular activity pattern, while general chemical properties of an odorant are reflected in the overall distribution of active modules. The properties of this coding strategy are incorporated in the model in Figure 6E. Furthermore, all glomerular modules responsive to AAs appear to be confined to a morphologically defined sub-region in the OB. Thus, there may be a further level of chemotopic organization in the OB that would presort information about general classes of odorants into sub-regions of the OB. Further testing of odorant classes is necessary to examine such a possible hierarchical sorting of information.

### Representation of Odorants by Patterns of Broadly Tuned Units: a Powerful and Nonrandom Coding Strategy

Combinatorial odor coding exhibits both similarities and differences to coding strategies used by other sensory systems. Unlike in other sensory systems, olfactory processing exhibits extensive parallel processing at the level of the sensory epithelium and the first relay station, the olfactory glomeruli. As odorant tuning of individual glomerular modules is broadly overlapping, the information processed in parallel appears to contain a high degree of redundancy, probably reflecting redundancy in OR-ligand interactions (Kauer, 1991; Shepherd, 1994). Such a strategy discards little information and may allow extraction of systematic molecular features of odorants that are inextractable at the level of ligand-OR interactions.

The coarse chemotopic map, which is established by the tendency for glomerular modules responding to certain principal molecular features to be located in common regions, resembles the organization of other sensory brain structures. Neighboring positions of units with similar response properties are a salient feature of sensory maps and are thought to provide an efficient organization for local computations, such as lateral inhibition, to be performed (Durbin and Mitchison, 1990).

Using presynaptic  $\text{Ca}^{2+}$  influx in ORNs as a marker for activity, we have characterized the organization of olfactory information specifically at the input level of the olfactory bulb. In contrast, many other studies have investigated odor coding in the OB at the output level by recording spikes from mitral cells. These studies have revealed correlations between structural features of odorants and mitral cell output (Meredith, 1981; Imamura et al., 1992; Mori et al., 1992; Katoh et al., 1993). Part of this tuning specificity of mitral cells is due to direct input from ORNs, while other components arise from computations within the olfactory brain, involving lateral inhibition (Scott et al., 1993; Yokoi et al., 1995). It will now be interesting to investigate how the patterned response of the array of glomerular modules is processed in the OB to generate spatiotemporal patterns of output activity, and to examine the underlying cellular mechanisms.

### Experimental Procedures

#### Dye Loading and Preparation

Adult zebrafish (*Danio rerio*) from our Tübingen institute stock (Ab/TU) were anesthetized in 0.01% MS-222, wrapped in a wet paper

towel, and kept under anesthesia by superfusion of the gills with 0.01% MS-222 through the mouth. A solution of 12% Calcium Green-1-dextran (10 kDa; Molecular Probes, Eugene, OR), 0.1% Triton X-100, and 1 mM NaCl in water (0.5–1.5  $\mu$ l per epithelium) was injected into the nasal cavities as described (Baier and Korsching, 1994) and washed out again after 4–6 min. Fish were then kept in separate tanks until they were used for experiments. For electron microscopy, epithelia were fixed in 2.5% glutaraldehyde for 24 hr and further processed by conventional techniques.

Following dye injection, physiological experiments were performed after a recovery and labeling period in vivo ( $\geq 2$  days for experiments with odorants). Dissection and subsequent manipulations were carried out in teleost artificial cerebrospinal fluid (ACSF) prebubbled with  $O_2$ - $CO_2$  (95%–5%) (Mathieson and Maler, 1988). For odorant stimulation, all structures caudal to the telencephalon and ventral from the OB and the telencephalon were removed such that an intact preparation of the olfactory system was obtained. The preparation was viewed ventrally with an inverted microscope (Axiocvert 100, Zeiss) and Zeiss filter set 17 (BP485/FT510/515–565) in a recording chamber that was constantly perfused with ACSF bubbled with  $O_2$ - $CO_2$  (95%–5%). Odorants were applied through a constant stream of ACSF (1–2 ml/min) directed at the inflow naris of one olfactory epithelium. Odorants were dissolved in ACSF and introduced into the constant stream using a motorized HPLC injection valve (Knauer, Germany). Operation of the valve was controlled and timed relative to image acquisition by computer. The time course of the stimulus consisted of an increase phase (1–3 s), a peak phase (0.5–1.5 s), and a falling phase (5–10 s), as monitored by application of a solution of a fluorescent dye (tetramethylrhodamine-dextran, 10 kDa). The stimulus conditions were constant throughout a given experiment and similar to those used previously in a study of electroolfactogram responses of zebrafish (Michel and Lubomudrov, 1995). Unless otherwise noted, AAs used were L-enantiomers. L-AAs were from Serva, D-Ala was from Sigma. Successive applications were separated by  $\geq 3$  min to exclude adaptation. For electrical stimulation, the olfactory nerve was stimulated with a suction electrode in an explant comprising the olfactory nerve, OB, and telencephalon. In  $Ca^{2+}$ -free ACSF,  $CaCl_2$  was replaced by 1 mM EGTA. Electrical stimulation of the olfactory nerve induces prominent signals in the OB after tracing is complete ( $\sim 8$  hr in vivo). Responses to AAs are weak initially ( $n = 2$ ) but prominent after  $\geq 2$  days when cilia have regenerated ( $n = 24$ ).

### Optical Imaging

Images (usually  $128 \times 128$  or  $170 \times 170$  pixel) were acquired with a cooled 12 bit CCD camera (PXL; Photometrics, Tucson, AZ) at 2–3.5 Hz in the frame transfer mode and corrected for dark current. Series of frames were corrected for bleaching by subtraction of a series obtained without stimulus. The time course of  $Ca^{2+}$  signals in glomerular modules consists of an increase, a peak, and a falling phase (Figure 3D) and generally parallels the time course of stimulus concentration. Images displaying relative changes in fluorescence are averages over 8–16 frames (constant for each preparation) from a single series, covering the increase, the peak, and part of the falling phase. All conditions concerning stimulus delivery, image acquisition, and data analysis were constant throughout a given experiment. For electrical stimulation, 1–4 s trains of pulses (200  $\mu$ s; 0.5–2 mA) were delivered through a suction electrode that was prepared to fit tightly the diameter of the olfactory nerve. Images displaying relative changes in fluorescence are averages over the stimulus period.

To observe activity in the entire OB, a  $10\times$  objective (NA 0.3; Zeiss) was used. Glomerular activity patterns in the subregion responsive to AAs were usually examined using a  $20\times$  objective (NA 0.5; Zeiss). In some cases, a  $40\times$  (NA 0.75; Zeiss) objective was also used to examine fine structures. To examine the structure of signals in three spatial dimensions, the same stimuli were reapplied with the focus set at different focal planes.

### Data Evaluation

AA stimuli were tested on a total of 26 preparations, including 17 males and 9 females. Experiments were performed  $\leq 1$  day ( $n = 2$ ), 2 days ( $n = 4$ ), 3 days ( $n = 10$ ), 4 days ( $n = 7$ ), or 5 days ( $n = 3$ )

after dye application. Because responses  $\leq 1$  day after dye application were weak, they were not included in further analysis. Glomerular activity patterns were examined in detail ( $\geq 20\times$  objective) in 22 of these preparations, and 11 preparations were tested with the full panel of 18 AAs. In most preparations, responses were examined at different focal planes and at different concentrations. For comparison across preparations, the anterior–posterior position of the imaged region was adjusted according to anatomical landmarks in the pattern of glomeruli. To determine the dorsoventral position, the depth of the lateral chain was determined prior to application of odorants by focusing and divided into three “z segments” of equal thickness. For analysis of glomerular activity patterns, data obtained within the middle z segment were used. By comparison with data obtained from the other z segments, we estimate that  $\sim 80\%$  of the total glomerular modules in the lateral chain can be imaged within the middle z segment. Given that an average of 95 glomerular modules is identifiable in the middle z segment with a high concentration of AAs, the total number of glomerular modules in the lateral chain is estimated to be  $\sim 120$ .

A focus of activity was considered to come from one glomerular module when it had a distinct appearance and responded uniformly to the panel of odorants. This criterion was verified by identification of the anatomical correlates for glomerular modules lying in the focal plane of imaging (see Figures 2C and 3B). When glomerular modules were somewhat out of focus, foci of activity were usually less distinct (Figure 2C). In this case, data from other z segments were consulted, which often allowed clearer delineation of foci of activity. Sometimes, especially when lying out of focus, signals from neighboring glomerular modules overlapped. In most cases, centers of highest signal intensity could be separated in overlapping foci, which were then taken as the positions of glomerular modules. Moreover, overlapping foci could usually be clearly separated, owing to their differential responses to the panel of odorants. However, it cannot be ruled out that, in some cases, closely apposed glomerular modules with similar response spectra were mapped as one module, which would result in an underestimation of the total number of glomerular modules. Such an underestimation would slightly disturb quantitative analysis but would not compromise the general results.

Statistical analysis was performed using StatView 4.5. and SPSS 6.0.1. The basis for statistical analysis is the matrix of stimuli versus modules. Intensity in glomerular modules was determined on an arbitrary scale from 0–4 spanning the intensities observed. In this matrix, the stimuli are viewed as vector variables that are determined by g elements (intensity values), with g being the total number of imaged glomerular modules.

Statistical results displayed are from data pooled for several preparations (see text and legends for exact numbers), except for those of Figures 6C and 6D. All analyses were performed also on the data from the individual preparations, which produced similar results, thus further supporting the similarities across individuals. Hierarchical clustering results displayed were obtained with single linkage (SPSS); other linkage methods produced similar results. Factor analysis results displayed were obtained with principal component extraction and orthotran–varimax transformation–rotation (StatView). This procedure first performs a principal component analysis and then relaxes the condition of orthogonality of factors to obtain the best fit. Other extraction and transformation–rotation methods produced similar results. The number of factors was determined according to the roots-greater-than-one criterion. Vectors representing factors were computed from the factor scores, which are the centered vector elements of factors. To scale these comparably to the original variables, the mean of each factor was added to the elements. This mean was obtained by summation of the means of the original variables weighted by the factor score weights for each factor (Rummel, 1970). Correlation of the factor vectors obtained with the original variables produced a correlation matrix identical to the oblique solution reference structure, thus confirming the validity of this calculation (Rummel, 1970; Bieber and Smith, 1986). The (hypothetical) activity patterns representing factors were then reconstructed by assigning the factor coordinate values to the respective glomerular modules in the original map.

## Acknowledgments

We are grateful to H. Baier, who participated in the development of the dye loading technique, and to F. Bonhoeffer for his support and continuing interest. We thank F. Weth for intense discussions, J. Lösinger for advice on electronics, J. Berger for expert assistance at the scanning electron microscope, and C. Nusslein-Volhard and colleagues for providing animals and zebrafish facilities. Thanks also to F. Weth, A. Borst, C. M. Müller, and C.-B. Chien for comments on the manuscript. R. W. F. was supported by a fellowship from the Boehringer Ingelheim Fonds. Correspondence should be addressed to R. W. F. (E-mail: fried@mpib-tuebingen.mpg.de).

Received February 25, 1997; revised March 21, 1997.

## References

- Adamek, G.D., Gesteland, R.C., Mair, R.G., and Oakley, B. (1984). Transduction physiology of olfactory receptor cells. *Brain Res.* 310, 87–97.
- Adrian, E.D. (1953). Sensory messages and sensation. *Acta Physiol. Scand.* 29, 5–14.
- Andres, K.H. (1970). Anatomy and ultrastructure of the olfactory bulb in fish, amphibia, reptiles, birds and mammals. In *Ciba Foundation Symposium on Taste and Smell in Vertebrates*, G.E.W. Wolstenholme and J. Knight, eds. (London: Churchill Press), pp. 177–196.
- Axel, R. (1995). The molecular logic of smell. *Sci. Am.* 273, 130–137.
- Baier, H., and Korsching, S. (1994). Olfactory glomeruli in the zebrafish olfactory system form an invariant pattern and are identifiable across animals. *J. Neurosci.* 14, 219–230.
- Barth, A.L., Justice, N.J., and Ngai, J. (1996). Asynchronous onset of odorant receptor expression in the developing zebrafish olfactory system. *Neuron* 16, 23–34.
- Bieber, S.L., and Smith, D.V. (1986). Multivariate analysis of sensory data: a comparison of methods. *Chem. Senses* 11, 19–47.
- Buck, L.B. (1996). Information coding in the vertebrate olfactory system. *Annu. Rev. Neurosci.* 19, 517–544.
- Buck, L., and Axel, R. (1991). A novel multigene family may encode odorant receptors: a molecular basis for odor recognition. *Cell* 65, 175–187.
- Byrd, C.A., and Brunjes, P.C. (1995). Organization of the olfactory system in the adult zebrafish: histological, immunohistochemical, and quantitative analysis. *J. Comp. Neurol.* 358, 247–259.
- Canalón, P. (1983). Influence of a detergent on the catfish olfactory mucosa. *Tissue Cell* 15, 245–258.
- Caprio, J. (1988). Peripheral filters and chemoreceptor cells in fishes. In *Sensory Biology of Aquatic Animals*, J. Atema, R.R. Fay, A.N. Popper, and W.N. Tavolga, eds. (Berlin: Springer), pp. 313–338.
- Caprio, J., and Byrd, R.J. (1984). Electrophysiological evidence for acidic, basic, and neutral amino acid olfactory receptor sites in the catfish. *J. Gen. Physiol.* 84, 403–422.
- Carr, W.E.S. (1988). The molecular nature of chemical stimuli in the aquatic environment. In *Sensory Biology of Aquatic Animals*, J. Atema, R.R. Fay, A.N. Popper, and W.N. Tavolga, eds. (Berlin: Springer), pp. 3–27.
- Chess, A., Simon, I., Cedar, H., and Axel, R. (1994). Allelic inactivation regulates olfactory receptor gene expression. *Cell* 78, 823–834.
- Cinelli, A.R., Hamilton, K.A., and Kauer, J.S. (1995). Salamander olfactory bulb neuronal activity observed by video rate, voltage-sensitive dye imaging. III. Spatial and temporal properties of responses evoked by odorant stimulation. *J. Neurophysiol.* 73, 2053–2071.
- Døving, K.B., Selset, R., and Thommesen, G. (1980). Olfactory sensitivity to bile acids in salmonid fishes. *Acta Physiol. Scand.* 108, 123–131.
- Durbin, R., and Mitchison, G. (1990). A dimension reduction framework for understanding cortical maps. *Nature* 343, 644–647.
- Firestein, S., Picco, C., and Menini, A. (1993). The relation between stimulus and response in olfactory receptor cells of the tiger salamander. *J. Physiol.* 468, 1–10.
- Getchell, T.V. (1986). Functional properties of vertebrate olfactory receptor neurons. *Physiol. Rev.* 66, 772–818.
- Guthrie, K.M., Anderson, A.J., Leon, M., and Gall, C. (1993). Odor-induced increases in c-fos mRNA expression reveal an anatomical “unit” for odor processing in olfactory bulb. *Proc. Natl. Acad. Sci. USA* 90, 3329–3333.
- Imamura, K., Mataga, N., and Mori, K. (1992). Coding of odor molecules by mitral/tufted cells in rabbit olfactory bulb. I. Aliphatic compounds. *J. Neurophysiol.* 68, 1986–2002.
- Ivanova, I., and Caprio, J. (1993). Odorant receptors activated by amino acids in sensory neurons of the channel catfish *Ictalurus punctatus*. *J. Gen. Physiol.* 102, 1085–1105.
- Kang, J., and Caprio, J. (1995). In vivo responses of single olfactory receptor neurons in the channel catfish, *Ictalurus punctatus*. *J. Neurophysiol.* 73, 172–177.
- Kato, K., Koshimoto, H., Tani, A., and Mori, K. (1993). Coding of odor molecules by mitral/tufted cells in rabbit olfactory bulb. II. Aromatic compounds. *J. Neurophysiol.* 70, 2161–2175.
- Kauer, J.S. (1991). Contributions of topography and parallel processing to odor coding in the vertebrate olfactory pathway. *Trends Neurosci.* 14, 79–85.
- Korsching, S., Argo, S., Campenhausen, H., Friedrich, R.W., Rummrich, A., and Weth, F. (1997). Olfaction in zebrafish: what does a tiny teleost tell us? *Semin. Cell. Dev. Biol.*, in press.
- Lancet, D., Greer, C.A., Kauer, J.S., and Shepherd, G.M. (1982). Mapping of odor-related neuronal activity in the olfactory bulb by high-resolution 2-deoxyglucose autoradiography. *Proc. Natl. Acad. Sci. USA* 79, 670–674.
- Levetau, J., and MacLeod, P. (1966). Olfactory discrimination in the rabbit olfactory glomerulus. *Science* 153, 175–176.
- Mathieson, W.B., and Maler, L. (1988). Morphological and electrophysiological properties of a novel in vitro preparation: the electrosensory lateral line lobe brain slice. *J. Comp. Physiol. [A]* 163, 489–506.
- Meredith, M. (1981). The analysis of response similarity in single neurons of the goldfish olfactory bulb using amino-acids as odor stimuli. *Chem. Senses* 6, 277–293.
- Michel, W.C., and Lubomudrov, L.M. (1995). Specificity and sensitivity of the olfactory organ of the zebrafish, *Danio rerio*. *J. Comp. Physiol. [A]* 177, 191–199.
- Mombaerts, P., Wang, F., Dulac, C., Chao, S.K., Nemes, A., Mendelsohn, M., Edmondson, J., and Axel, R. (1996). Visualizing an olfactory sensory map. *Cell* 87, 675–686.
- Mori, K., Mataga, N., and Imamura, K. (1992). Differential specificities of single mitral cells in rabbit olfactory bulb for a homologous series of fatty acid odor molecules. *J. Neurophysiol.* 67, 786–789.
- Moulton, D.G. (1967). Spatio-temporal patterning of response in the olfactory system. In *Olfaction and Taste II*, T. Hayashi, ed. (New York: Pergamon Press), pp. 109–116.
- Ngai, J., Dowling, M.M., Buck, L., Axel, R., and Chess, A. (1993). The family of genes encoding odorant receptors in the channel catfish. *Cell* 72, 657–666.
- Oka, Y., Ichikawa, M., and Ueda, K. (1982). Synaptic organization of the olfactory bulb and central projection of the olfactory tract. In *Chemoreception in Fishes*, T.J. Hara, ed. (Amsterdam: Elsevier), pp. 61–75.
- Ressler, K.J., Sullivan, S.L., and Buck, L.B. (1994a). Information coding in the olfactory system: evidence for a stereotyped and highly organized epitope map in the olfactory bulb. *Cell* 79, 1245–1255.
- Ressler, K.J., Sullivan, S.L., and Buck, L.B. (1994b). A molecular dissection of spatial patterning in the olfactory system. *Curr. Opin. Neurobiol.* 4, 588–596.
- Reval, M.F., Sicard, G., Duchamp, A., and Holley, A. (1982). New studies on odour discrimination in the frog's olfactory receptor cells. I. Experimental results. *Chem. Senses* 7, 175–190.

- Rhein, L.D., and Cagan, R.H. (1983). Biochemical studies of olfaction: binding specificity of odorants to a cilia preparation from rainbow trout olfactory rosettes. *J. Neurochem.* **41**, 569–577.
- Riddle, D.R., and Oakley, B. (1992). Immunocytochemical identification of primary olfactory afferents in rainbow trout. *J. Comp. Neurol.* **324**, 575–589.
- Rummel, R.J. (1970). *Applied Factor Analysis*. (Evanston: Northwestern University Press).
- Satou, M. (1992). Synaptic organization of the olfactory bulb and its central projections. In *Fish Chemoreception*, T.J. Hara, ed. (London: Chapman and Hall), pp. 40–59.
- Scott, J.W., Wellis, D.P., Riggott, M.J., and Bounviso, N. (1993). Functional organization of the main olfactory bulb. *Microsc. Res. Tech.* **24**, 142–156.
- Shepherd, G.M. (1994). Discrimination of molecular signals by the olfactory receptor neuron. *Neuron* **13**, 771–790.
- Shipley, M.T., and Ennis, M. (1996). Functional organization of olfactory system. *J. Neurobiol.* **30**, 123–176.
- Stewart, W.B., Kauer, J.S., and Shepherd, G.M. (1979). Functional organization of rat olfactory bulb analysed by the 2-deoxyglucose method. *J. Comp. Neurol.* **185**, 715–734.
- Strader, C.D., Fong, T.M., Tota, M.R., and Underwood, D. (1994). Structure and function of G protein-coupled receptors. *Annu. Rev. Biochem.* **63**, 101–132.
- Treloar, H., Walters, E., Margolis, F., and Key, B. (1996). Olfactory glomeruli are innervated by more than one distinct subset of primary sensory neurons in mice. *J. Comp. Neurol.* **367**, 550–562.
- Vassar, R., Chao, S.K., Sitcheran, R., Nunez, J.M., Vosshall, L.B., and Axel, R. (1994). Topographic organization of sensory projections to the olfactory bulb. *Cell* **79**, 981–991.
- Weth, F., Nadler, W., and Korsching, S. (1996). Nested expression domains for odorant receptors in zebrafish olfactory epithelium. *Proc. Natl. Acad. Sci. USA* **93**, 13321–13326.
- Yokoi, M., Mori, K., and Nakanishi, S. (1995). Refinement of odor molecule tuning by dendrodendritic synaptic inhibition in the olfactory bulb. *Proc. Natl. Acad. Sci. USA* **92**, 3371–3375.
- Zippel, H.P., Voigt, R., Knaust, M., and Luan, Y. (1993). Spontaneous behavior, training and discrimination training in goldfish using chemosensory stimuli. *J. Comp. Physiol. [A]* **172**, 81–90.